℘

Level Splitting at Macroscopic Scale

A. Eddi,[1] J. Moukhtar,[1] S. Perrard,[1] E. Fort,[2] and Y. Couder[1]

[1]*Laboratoire Matière et Systèmes Complexes, Université Paris Diderot, CNRS—UMR 7057, Bâtiment Condorcet,*
10 rue Alice Domon et Léonie Duquet, 75013 Paris, France
[2]*Institut Langevin, ESPCI ParisTech and Université Paris Diderot, CNRS—UMR 7587,*
10 rue Vauquelin, 75231 Paris Cedex 05, France

A walker is a classical self-propelled wave particle association moving on a fluid interface. Two walkers can interact via their waves and form orbiting bound states with quantized diameters. Here we probe the behavior of these bound states when setting the underlying bath in rotation. We show that the bound states are driven by the wave interaction between the walkers and we observe a level splitting at macroscopic scale induced by the rotation. Using the analogy between Coriolis and Lorentz forces, we show that this effect is the classical equivalent to Zeeman splitting of atomic energy levels.

PACS numbers: 47.55.D−, 05.45.−a, 05.65.+b, 32.60.+i

The possibility of analogies between quantum waves and fluid surface waves was first shown to be relevant and useful by M. Berry *et al.* [1] when these authors gave an intuitive interpretation of the Aharonov-Bohm effect [2]. Until then, this quantum effect had been considered strange: electrons traveling outside a solenoid containing a magnetic field are scattered even though they travel in magnetic-field-free regions of space. Berry *et al.* showed that this effect is linked with the formation of a dislocation in the front of the Schrödinger wave. These authors then used the formal similarity that exists in classical physics between the effect of rotation on moving masses and the effect of a magnetic field on moving charges. With this analogy they showed that the same type of dislocation is created in the fronts of surface waves when they meet a vortex. In this system, the equivalent of the vector potential is the fluid velocity and the formation of the dislocation is simply ascribed to the different advection of the wave front on both sides of the vortex. This effect has now been thoroughly investigated for surface waves [3,4] as well as for acoustic waves [5].

An even larger range of possible analogies between quantum physics and fluid mechanics was opened when a hydrodynamic system presenting wave-particle duality at macroscopic scale was introduced. Using walkers, quantumlike single particle diffraction and interferences were observed [6] as well as a tunneling effect [7]. Two walkers were also shown to form orbiting bound states with discrete diameters.

In this Letter, we study the behavior of bound states of two walkers when submitted to an external field. Using the analogy introduced by Berry *et al.* [1], we compare our results to the effect of a magnetic field on atomic orbits. We demonstrate that we can induce splitting of the macroscopic levels, reminiscent of Zeeman splitting as well as transition in between levels.

Experiments.—As described in [8,9], a drop can bounce on the surface of a vertically vibrated liquid bath: at each

oscillation, the air film squeezed between the two fluids has no time to break before the drop lifts off again. At each bounce, the drop emits surface waves. For large forcing accelerations the drop bounces with the Faraday frequency f_F and emits surface waves with the Faraday wavelength $\lambda_F = 4.75$ mm, in agreement with the value predicted by the dispersion relation for surface waves. In this regime, below but close to the Faraday instability threshold, the waves are weakly damped. The drop then couples to its own waves and starts moving spontaneously on the interface with a constant velocity V_w [9]. This is a drift bifurcation so that the initial direction of motion is random. The object formed by the drop and its associated wave was called a *walker.*

We create two identical walkers and let them evolve on the bath surface. When close enough, they interact through the emitted waves. They bind to each other, each drop being trapped in the wave field created by its partner [see Figs. 1(a) and 1(b)]. Both walkers then follow circular orbits, the direction of rotation being set by the initial collision conditions. The orbit diameter of such a bound state is discrete and scaled on the Faraday wavelength λ_F. We recall that the drops bounce at the Faraday frequency f_F, which is half the forcing frequency f_0. For this reason each drop can have two possible phases and a pair of drops can have either a synchronous bouncing or have opposite phases; two families of bound states are thus observed. The orbit diameters are given by [9]:

$$d_n = (n - \epsilon_0)\lambda_F \tag{1}$$

where $\epsilon_0 = 0.21$ and n is an integer if the drops are in phase ($n = 1, 2, \ldots$), a half-integer if they are of opposite phases ($n = \frac{1}{2}, \frac{3}{2} \ldots$). We also measured V_n the walkers velocity orbiting on the nth bound state. It is minimal for $n = 1/2$ and slowly increases with n asymptotically reaching the free velocity of the walker. The minimal speed $V_{1/2}$ is about 20% smaller than V_w.
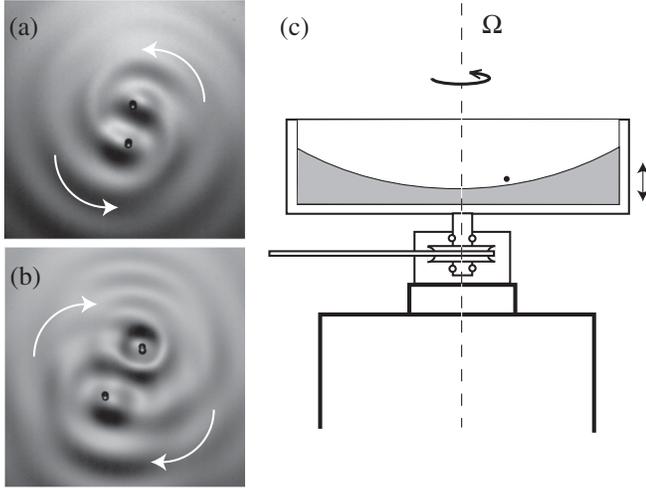
FIG. 1. (a) Snapshot of two counterclockwise orbiting walkers with $n^+ = (1)^+$. (b) Snapshot of two walkers orbiting clockwise with $n^- = (1.5)^-$. (c) Sketch of the experimental setup. A silicon oil bath with viscosity $\mu = 20 \times 10^{-3}$ Pa $\cdot$ s, density $\rho = 965$ kg $\cdot$ m^{-3} and surface tension $\sigma = 20.9$ mN $\cdot$ m^{-1} is subjected to a sinusoidal vertical acceleration $\gamma = \gamma_m \sin 2\pi f_0 t$. The forcing frequency is $f_0 = 80$ Hz. We create the drops by removing swiftly a needle from the bath as described in [10]. They have a diameter $D_G = 0.8$ mm and a mass m_G. The angular velocity Ω can be tuned with a motor.

As shown on Fig. 1(c), the cell can be set into counterclockwise rotation at an angular velocity Ω, ranging from 0 to 5 Hz. Note that there are two possible states for each value of n: the corotating state that we will denote n^+ and the counterrotating one that we will denote n^-. In our experiments, the bath is rotating counterclockwise, thus n^+ orbits are rotating counterclockwise, n^- clockwise. Two examples of these orbits are shown. Figure 1(a) is a $n^+ = (1)^+$ orbit and Fig. 1(b) is $n^- = (1.5)^-$.

The trajectories of the two drops are recorded in the laboratory frame of reference when the bath is set into rotation. Both are epicycles [Fig. 2(a)]. From these data, the trajectories in the rotating frame can be reconstructed and they are found to be circular. The vector $\vec{d}$ joining the two walkers has a constant modulus $d_n(\Omega)$ and rotates with a constant angular velocity ω_{orb} [see Fig. 2(b)]. We observe that the velocity V_n of the walkers is constant and does not depend on Ω. Two cases must be distinguished, depending on the sign of the orbital motion. When the orbit and the bath are contrarotative (n^+) the motion of the two drops is slowed in the laboratory frame, the orbit is stabilized and its diameter decreases. In the corotative case (n^-), the increase of Ω leads to an increase of the orbit diameter and a higher angular velocity in the laboratory frame. When a limit value of Ω is reached, the (n^-) orbital state becomes unstable and breaks down.

We repeated this experiment using all the possible orbits of order n of the two drops. The evolution of the diameters d_n with respect to Ω are shown in Fig. 2(c). We observe
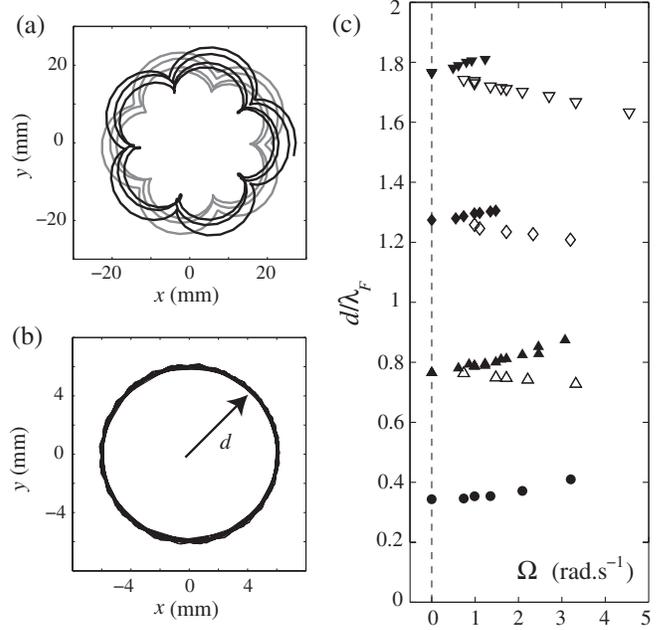

FIG. 2. (a) Recorded trajectory in the laboratory frame of reference for two walkers on a $n^- = (1.5)^-$ level and $\Omega = 0.99$ rad $\cdot$ s^{-1}. (b) Time evolution of the vector $\vec{d}$ joining the two walkers showing the diameter of the orbit. $\vec{d}$ has a constant modulus and rotates with a constant angular velocity $\omega_{\mathrm{orb}} = 5.44$ rad $\cdot$ s^{-1}. (c) The evolution of the diameters d_n with respect to Ω for different values of n. The open symbols correspond to contrarotation (n^-), the black ones to corotation (n^+).

experimentally that all the d_n vary linearly with Ω: they decrease for all the n^- and increase for all the n^+ states. The observed slope increases with n. In the following we write that $d_n(\Omega) = d_n(0) + \delta_n(\Omega)$ where δ_n is the shift relative to the diameters observed in the absence of rotation.

Probing the binding force.—We use the external field Ω as a control parameter to probe the interaction force between two walkers. Without rotation, the diameters d_n are given by a balance between the centrifugal force $F_c = 2m_G V_n^2 / d_n$ and the wave mediated interaction force F_{int}. When the bath is set in rotation, the Coriolis force $F_{\mathrm{Cor}} = 2m_G \Omega V_n$ orthogonal to motion modifies this equilibrium. The shift δ_n can be related to a new equilibrium between F_{int}, F_c and F_{Cor}. As the rotation does not induce any change of V_n, δ_n induces a typical variation of the centrifugal force $\delta F_c < 8 \times 10^{-8}$ N which is smaller than the applied Coriolis force $F_{\mathrm{Cor}} \simeq 2 \times 10^{-7}$ N. Thus, we can neglect the variation of F_c and we obtain a simple expression for F_{int}:

$$F_{\mathrm{int}}(d_n + \delta_n) = 2m_G \left(\Omega V_n + \frac{V_n^2}{d_n} \right). \qquad (2)$$

The deduced value of F_{int} from the experimental data is shown in Fig. 3(a). We observe that F_{int} oscillates with the same wavelength as the surface waves.
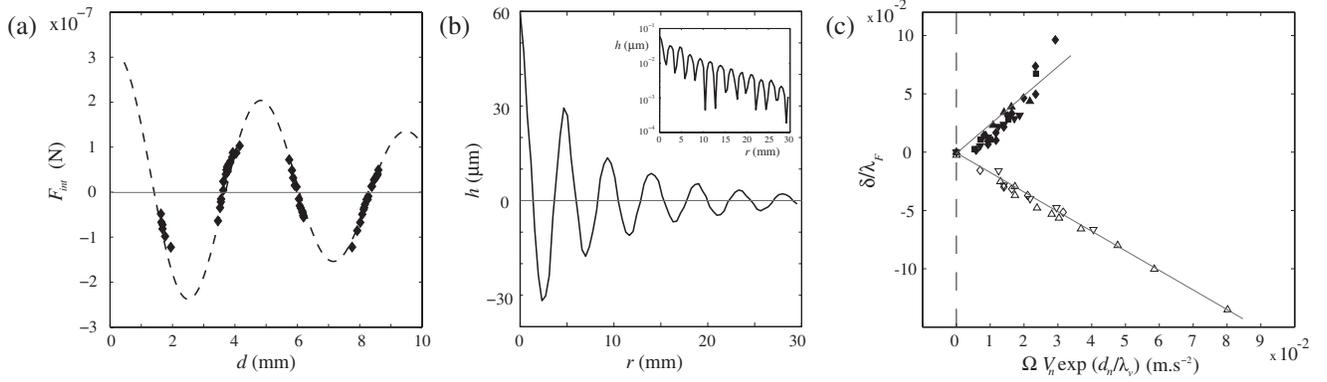
FIG. 3.   (a) Measured interaction force F_{int} as a function of d. The dashed line is a guide for the eye. (b) Experimental measurements of the wave created by a walker in the direction orthogonal to motion. The inset in semilogarithmic scale shows an exponential decay of the wave. The characteristic length of decay is $l_\nu \simeq 2\lambda_F$. (c) Experimental data δ_n as a function of Ω with the scaling given by Eq. (5). All data collapse on the same master curve.

The interaction between the two walkers is related to the shape of the wave field they generate [9,10]. Using a synthetic schlieren technique [11], the surface height $h(d)$ has been measured in the direction orthogonal to motion for a free walker [see Fig. 3(b)]. It has a spatial pseudoperiod λ_F and decays exponentially because of viscous damping with a characteristic damping length $l_\nu \simeq 2\lambda_F$. A phenomenological model gives a good estimate of the interaction force including the slope of the surface at the bouncing point [9]:

$$F_{\mathrm{int}}(d) = m_G \gamma_m \frac{\tau}{\tau_F} \vec{\nabla} h(d) \sim m_G \gamma_m \frac{\tau}{\tau_F} \frac{A_w}{\lambda_F} \qquad (3)$$

with τ/τ_F the ratio between contact time τ during bouncing and Faraday period τ_F and A_w the amplitude of the surface wave. Typical values are $\gamma_m = 5$ g, $\tau/\tau_F \sim 0.2$, and $A_w/\lambda_F \sim 0.01$. This leads to $F_{\mathrm{int}} \sim 2 \times 10^{-7}$ N, in good agreement with the measured amplitude of the force. We thus assume that one can write:

$$F_{\mathrm{int}} = F_0 \exp(-d/l_\nu) \sin\!\left(\frac{2\pi d}{\lambda_F} + \varphi\right). \qquad (4)$$

Such an expression for F_{int} allows for the numerical simulations of discrete orbits of walkers [9], but also of quantized self-orbits [12]. From this description we can deduce a theoretical scaling for the shift δ with a linear dependency in Ω. Expanding Eq. (2) with Eq. (4) we get:

$$\frac{\delta}{\lambda_F} = \frac{m_G}{\pi F_0} \Omega V_n \exp\!\left(\frac{d_n}{l_\nu}\right). \qquad (5)$$

Figure 3(c) shows the experimental data rescaled using this expression. This scaling provides a good collapse of the diameter shift for each n bound state. The predicted slope $m_G/(\pi F_0) \simeq 3$ m$^{-1} \cdot$ s^2 is in qualitative agreement with the experimental one [see Fig. 3(c)], confirming the validity of the previous analysis. The observed scaling is linked with the spatial decay of the waves due to viscosity. Note

that in a nondissipative system, the spatial decay would be given by Bessel functions, changing the final scaling.

Analogy with Zeeman splitting.—The relation $2\boldsymbol{\Omega} = \boldsymbol{\nabla} \times \mathbf{U}$ between the fluid velocity $\mathbf{U}$ and the vorticity $\boldsymbol{\Omega}$ corresponds to $\mathbf{B} = \boldsymbol{\nabla} \times \mathbf{A}$ in electromagnetism [1]. The magnetic field $\mathbf{B}$ is thus formally equivalent to the vorticity $2\boldsymbol{\Omega}$ and the vector potential $\mathbf{A}$ corresponding to the velocity field $\mathbf{U}$ of the waves.

Our experiments show that, for a system of two drops with a angular momentum $L_n^\pm = \pm m_G d_n V_n$, an external rotation Ω induces a linear shift of the orbit diameter $d_n(\Omega)$. Using the correspondence of the equations between fluid mechanics and electromagnetism, we seek a similar situation in the quantum world. Our system turns out to be equivalent to a rotating electrical charge e subjected to a constant magnetic field $\mathbf{B}$. In that case, it is possible to define a magnetic interaction energy:

$$E_{\mathrm{mag}} = \frac{e}{2m_e} \mathbf{L} \cdot \mathbf{B} \qquad (6)$$

where m_e denotes the mass of the particle and L its angular momentum. If we consider an electron with an energy level E with a characteristic frequency $\omega_E = E/\hbar$ the magnetic interaction induces a shift frequency $\delta\omega_E$ given by:

$$\delta\omega_E = \frac{e}{2m_e} \frac{\mathbf{L} \cdot \mathbf{B}}{\hbar}. \qquad (7)$$

This effect is responsible for Zeeman splitting in quantum mechanics [13]: two states with different values of $\mathbf{L}$ will have different characteristic frequency when $\mathbf{B} \neq 0$. In our classical system, we can also define a potential energy $E_{\mathrm{Cor}} = 2\mathbf{L}_n \cdot \boldsymbol{\Omega}$ for a walker submitted to a vorticity Ω. As the potential energy E_{Cor} is formally equivalent to E_{mag}, our experimental results directly compare to Zeeman splitting. Each orbital level of the discrete set $n = 1/2, 1, 3/2, 2, \ldots$ can have two symmetrical states $L_n^\pm$. When no external field is applied, these two states cannot be physically distinguished. When $\Omega \neq 0$, the system is
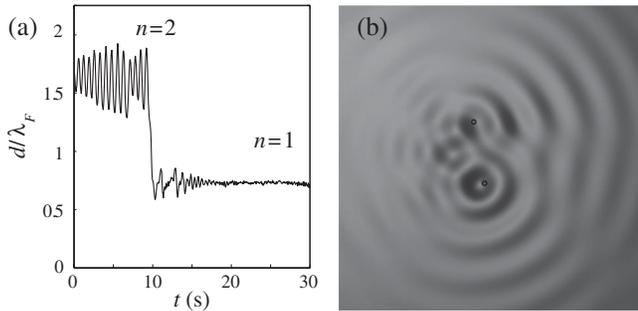
FIG. 4.   (a) Evolution of the adimensional distance d/λ_F between two walkers for a rotation rate $\Omega = 4.3$ rad $\cdot$ s^{-1}. After transient oscillations, we observe an abrupt transition from $n = 2$ to $n = 1$. (b) Snapshot of the complex structure of the unsteady wave field during the transition.

plunged into a potential $2\mathbf{L}_n \cdot \mathbf{\Omega}$ and we observe a linear shift δ_n, with the sign of this shift determined by the sign of the energy variation. We can compute the rotation frequency $\omega_n(\Omega) = V_n/d_n(\Omega)$ and expand this expression at first order to get the frequency shift $\delta\omega_n^\pm$:

$$\delta\omega_n^\pm = \frac{V_n \delta_n(\Omega)}{d_n(0)^2}. \qquad (8)$$

From Eq. (5), $\delta\omega_n^\pm$ can be written as a linear function of the external field Ω:

$$\delta\omega_n^\pm = \pm\alpha_n\Omega \qquad (9)$$

where α_n depends only on the order n of the binding level. We thus have an analogy with Zeeman splitting. Here, the shift depends exponentially on the order n of the level while it is linear in quantum mechanics. This major difference might be related to the nature of the quantization in both cases: in quantum mechanics energy and frequency are quantized while the wave interaction leads to a quantized distance between the walkers.

Interlevel transitions.—Can we use the external potential E_{Cor} to modify the bound state? We prepare a $n^- = (2)^-$ orbit, and submit it to an intense counterrotation. The distance between the two drops first decreases according to Eq. (5) and then presents some oscillations [Fig. 4(a)]. For a large enough value of Ω, these oscillations are amplified and the level $n = 2$ becomes unstable: the distance between the two walkers decreases abruptly, and they settle on the $n = 1$ level. During the transition, the wave field around the two walkers present a strong asymmetry [see Fig. 4(b)]. Note that such transitions are subject to selection rules. The direction of rotation is preserved, so that transitions from levels n^- to n^+ are forbidden. Similarly, the relative phase of the two bouncing drops is also preserved so that transitions are forbidden between integer and

semi-integer orders: a drop cannot transit from $n = 2$ to $n = 3/2$. When the two drops are bouncing in phase, the $n = 1$ level is the fundamental level, while it is $n = 1/2$ for opposite phase drops. The oscillations observed prior to transition could be analogous to Rabi oscillations in between two resonant levels. Both the oscillations observed before the transition and the structure of the waves emitted during the transitions should be studied in order to understand the very nature of these events. We reserve these studies for future work.

Conclusion.—Two walkers can form quantized orbiting bound states when they interact. Here we have probed the properties of this set of orbits when submitted to an external field. We have shown that the wave mediated interaction is dominant over inertial effects, and that the bound states present a strong analogy with atomic systems. An external field induces a level splitting of degenerate states, reminiscent of Zeeman splitting, and is also able to force transitions between successive levels. The present results have thus extended the range of the documented analogies between phenomena due to wave-particle duality at classical and quantum scales, respectively. The existence of these behavioral similarities opens a new perspective for the understanding of both types of dualities.

[1] M. V. Berry, R. G. Chambers, M. D. Large, C. Upstill, and J. C. Walmsley, Eur. J. Phys. **1**, 154 (1980).
[2] Y. Aharonov and D. Bohm, Phys. Rev. **115**, 485 (1959).
[3] F. Vivanco, F. Melo, C. Coste, and F. Lund, Phys. Rev. Lett. **83**, 1966 (1999).
[4] C. Coste, F. Lund, and M. Umeki, Phys. Rev. E **60**, 4908 (1999).
[5] P. Roux, J. de Rosny, M. Tanter, and M. Fink, Phys. Rev. Lett. **79**, 3170 (1997).
[6] Y. Couder and E. Fort, Phys. Rev. Lett. **97**, 1 (2006).
[7] A. Eddi, E. Fort, F. Moisy, and Y. Couder, Phys. Rev. Lett. **102**, 240401 (2009).
[8] Y. Couder, S. Protiere, E. Fort, and A. Boudaoud, Nature (London) **437**, 208 (2005).
[9] S. Protiere, A. Boudaoud, and Y. Couder, J. Fluid Mech. **554**, 85 (2006).
[10] A. Eddi, E. Sultan, J. Moukhtar, E. Fort, M. Rossi, and Y. Couder, J. Fluid Mech. **674**, 433 (2011).
[11] F. Moisy, M. Rabaud, and K. Salsac, Exp. Fluids **46**, 1021 (2009).
[12] E. Fort, A. Eddi, J. Moukhtar, A. Boudaoud, and Y. Couder, Proc. Natl. Acad. Sci. U.S.A. **107**, 17515 (2010).
[13] P. Zeeman, Philos. Mag. **43**, 226 (1897).